

# First determination of the (re)crystallization activation energy of an irradiated olivine-type silicate

Z. Djouadi<sup>1</sup>, L. d’Hendecourt<sup>1</sup>, H. Leroux<sup>2</sup>, A. P. Jones<sup>1</sup>, J. Borg<sup>1</sup>, D. Deboffe<sup>1</sup>, and N. Chauvin<sup>3</sup>

<sup>1</sup> IAS – CNRS, “Astrochimie Expérimentale”, Université Paris XI, Bâtiment 121, 91405 Orsay Cedex, France  
e-mail: zahia.djouadi@ias.u-psud.fr

<sup>2</sup> LSPES ESA CNRS 8008, Université des Sciences et Technologies de Lille, Bâtiment C6,  
59655 Villeneuve d’Ascq Cedex, France

<sup>3</sup> CSNSM, Université Paris XI, Bâtiment 108, 91405 Orsay Cedex, France

Received 19 April 2005 / Accepted 13 May 2005

**Abstract.** To study the evolution of silicate dust in different astrophysical environments we simulate, in the laboratory, interstellar and circumstellar ion irradiation and thermal annealing processes. An experimental protocol that follows different steps in the dust life-cycle was developed. Using the silicate 10  $\mu\text{m}$  band as an indicator, the evolution of the structural properties of an ion-irradiated olivine-type silicate sample, as a function of temperature, is investigated and an activation energy for crystallization is determined. The obtained value of  $E_a/k = 41\,700 \pm 2400$  K is in good agreement with previous determinations of the activation energies of crystallization reported for non-ion-irradiated, amorphous silicates. This implies that the crystallization process is independent of the history of the dust. In particular, the defect concentration due to irradiation appears not to play a major role in stimulating, or hindering, crystallization at a given temperature. This activation energy is an important thermodynamical parameter that must be used in theoretical models which aim to explain the dust evolution from its place of birth in late type stars to its incorporation into young stellar environments, proto-stellar discs and proto-planetary systems after long passage through the interstellar medium.

**Key words.** methods: laboratory – techniques: spectroscopic – ISM: dust, extinction

## 1. Introduction

The structural and chemical evolution of silicate grains in the interstellar medium (ISM) is not yet well understood. Previous to the observations made by the ISO-SWS instrument, it was largely believed that all silicate dust in space was completely amorphous. The extensive spectroscopic results provided by ISO showed the presence of crystalline dust in evolved star outflows (Waters et al. 1996; Molster et al. 2002), some comets (Crovisier et al. 1997; Wooden et al. 1999, 2004), young stellar environments (Malfait et al. 1998, 1999) and the co-existence of both amorphous and crystalline silicate phases in AGB M-type stellar envelopes (Kemper et al. 2001). However, a recent upper limit of 1% on the abundance of crystalline silicates in the ISM was determined (Kemper et al. 2004), a result which confirms the determination of the relative abundance of crystalline materials in two protostellar objects (Demyk et al. 1999). This result thus shows that most, if not all, of the silicate material towards young protostars is of an amorphous nature. In order to explain the ISO observations, termed “the crystalline revolution” (Jäger et al. 1998), many experimental studies have been devoted to understanding the interstellar silicate dust evolution under the effects of ion irradiation (Demyk et al. 2001; Carrez et al. 2002; Jäger et al. 2003; Brucato et al. 2004; Demyk et al. 2004) or thermal annealing

(Hallenbeck et al. 1998; Brucato et al. 2002). Some of these studies demonstrate that the ion irradiation of crystalline silicates rather efficiently leads to their amorphization. This process could thus explain the absence of crystalline silicate in the ISM, since energetic ion fluences similar to those used in the laboratory simulations are expected during the passage of grains through shock waves in the ISM (Demyk et al. 2001). Indeed, from a theoretical point of view, it is reasonable to assume that the crystalline silicates around evolved stars are injected into the ISM and are then subsequently amorphized by ion implantation in the supernovae shock waves and stellar winds that permeate this environment (e.g., Jones 2000).

If a number of studies have been devoted to the structural modification of silicates under the effects of ion irradiation, little has been done on the further evolution of these irradiated silicates, in particular when the dust is involved in the formation of new stars. During this stage the dust temperature may significantly increase and lead to some crystallization of the amorphous ISM precursors. The role of any such previous irradiation in modifying the thermodynamical properties of the grains has not yet been considered.

The aim of this paper is to evaluate the influence of ion irradiation on the activation energy of crystallization for silicates. If correctly constrained, such a parameter could be used

in theoretical models describing grain evolution in the ISM. In Sect. 2 we describe the experimental and analytical procedures used. The results obtained are discussed in Sect. 3 and we present our conclusions in Sect. 4.

## 2. Experimental methods

### 2.1. Sample preparation

The laboratory synthesis of interstellar dust analogs includes several techniques that aim to simulate the formation conditions and the further processing of these solid materials (see Colangeli et al. 2003, for an extensive review). These techniques include reactive thermal evaporation (Rietmeijer et al. 1999), laser ablation (Brucato et al. 1999), sol-gel synthesis (Jäger et al. 2003), ion sputtering (Hanley & Sinnott 2002) and laser pyrolysis (Herlin et al. 1998). The samples that we analyse in our work were prepared by electron-beam evaporation in a high vacuum chamber ( $10^{-7}$  mbar). This provides an efficient way to prepare thin amorphous films having a high surface-to-volume ratio analogous to interstellar dust grains. The electrons from a tungsten filament are focussed onto a crucible containing the evaporating material source by means of electromagnets. We used the San Carlos olivine ( $\text{Mg}_{1.8}\text{Fe}_{0.2}\text{SiO}_4$ ) as the solid precursor. The target material is heated by the high current density electron beam and is locally transformed into liquid. The atoms gain enough vibrational kinetic energy to escape from the target in the form of a vapour and are transported directly to the substrate in the high vacuum in the chamber. The working pressure was typically between  $10^{-7}$  and  $10^{-6}$  mbar, low enough to ensure a long mean free path for the atoms ( $\sim 30$  cm). The vapour deposition rate was maintained at between 0.2 and 0.5 Å/s. A low deposition rate was chosen to avoid an increase in the background pressure of the chamber. The deposition rate and final film thickness were controlled with a quartz micro balance. The substrate on which the vapour is deposited is a bevelled ( $\sim 1^\circ$ ) 3 mm diameter and 0.25 mm thickness diamond window (Rent-Optic, France). Diamond has the double advantage of a good resistance to high temperature (under vacuum) and good IR transparency in the 4000–250  $\text{cm}^{-1}$  range used in our experiments.

### 2.2. Experimental protocol

The thin samples prepared by evaporation are amorphous, as verified by IR spectroscopy. However the exact chemical composition can not be determined from only IR spectroscopy because of the broadness of the bands and the uncertainties in the band position, which is the relevant parameter for the nature of minerals.

To obtain very thin films (of the order of 100 nm at most) of crystalline silicates analogous to the dust detected in asymptotic giant branch (AGB) stellar atmospheres, we must then crystallize the thin films by heating them at 1050 °C for 30 min. This allows a verification of the silicate mineralogy via IR spectroscopy.

A re-amorphization of the thin films of crystalline silicates, of known chemical composition and mineralogy, is then

achieved by  $\text{He}^+$  ion irradiation. This simulates an ion irradiation process that could be responsible for modifying the dust structure in the interstellar medium in supernova shock waves. Finally, the sample is recrystallized by controlled step annealing, a process that could be analogous to that occurring in the vicinity of newly-forming young stars and planetary systems. Each step throughout the entire process is monitored by IR spectroscopy.

### 2.3. Instrumentation and experimental details

The silicate annealing was performed in a tubular furnace under vacuum (generally between  $10^{-7}$  and  $10^{-6}$  mbar). The temperature inside the quartz tube furnace used for the annealing was measured with a thermocoaxial thermocouple (chromel-Alumel). The error in the temperature measurement was less than 5%.

The sample irradiation was performed at the isotope separator facility, SIDONIE, in Orsay (Chauvin et al. 2004). The  $\text{He}^+$  beam is first accelerated to an energy of 40 keV and then electrostatically decelerated to the desired energy just before impact with the sample. In order to avoid excessive sample heating, the beam current was kept below 10  $\mu\text{A}$ . The irradiations were performed under vacuum ( $10^{-7}$  mbar) and at room temperature. The  $\text{He}^+$  doses implanted into the samples were  $10^{17}$  at/ $\text{cm}^2$  at an incident energy of 5 keV and  $5 \times 10^{16}$  at/ $\text{cm}^2$  at an energy of 10 keV. These conditions, based on the results obtained from previous experiments (Demyk et al. 2001), ensure total amorphization of the samples after irradiation.

### 2.4. Analytical technique

IR spectroscopy is a very sensitive tool for the study of the structural modifications in analyzed samples and it also allows a direct comparison with astronomical observations. The spectroscopy was performed with a Bruker IFS 66V IR Fourier transform interferometer. The configuration used consisted of a Globar (black body-like) source coupled with a CsI beam-splitter and a Deuterated TriGlycine Sulfate (DTGS) detector. All the spectra were obtained in the range 4000–250  $\text{cm}^{-1}$  (2.5–40  $\mu\text{m}$ ) with a spectral resolution of 4  $\text{cm}^{-1}$ .

## 3. Results and discussion

In Fig. 1 we show three plots of the absorbance (in absorbance units, a.u.) versus wavelength ( $\mu\text{m}$ ). The plots show the IR spectra obtained after evaporation of the San Carlos olivine and deposition as a thin film on the diamond substrate (Fig. 1a), after annealing at 1050 °C for 30 min (Fig. 1b) and after  $\text{He}^+$  irradiation (Fig. 1c). Displaying the entire spectral region shows that the diamond substrate does not show any changes after thermal annealing and  $\text{He}^+$  irradiation. The plots show the well-known two-phonon transitions of the diamond lattice (Vogelgelsang et al. 1998) in the wavenumber range 2700–1600  $\text{cm}^{-1}$  (3.7–6.25  $\mu\text{m}$ ). The main silicate bands occur at  $\sim 10$  and  $\sim 18$ –20  $\mu\text{m}$ , therefore diamond represents a suitable substrate for annealing experiments because we can easily

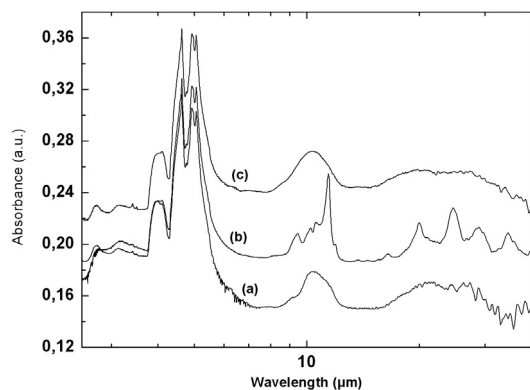


**Fig. 1.** The IR signatures of the olivine-type silicate plotted as absorbance versus wavelength 2.5–40  $\mu\text{m}$  (4000–250  $\text{cm}^{-1}$ ) for: **a)** the deposited electron beam thin film, **b)** the thin film crystallized after annealing at 1050  $^{\circ}\text{C}$  for 30 min and **c)** the amorphized sample after irradiation by an  $\text{He}^{+}$  beam at an energy of 5 keV and a fluence of  $10^{17}$   $\text{at}/\text{cm}^2$ .

distinguish between the signatures due to the substrate and those due to the deposited silicate.

The data in Fig. 1 highlight the crystalline silicate band growth from (a) to (b), particularly for the 10  $\mu\text{m}$  band, and the disappearance of the crystalline silicate bands after ion irradiation (b) to (c).

The broad bands at  $\sim 10$  and  $\sim 20$   $\mu\text{m}$  in the spectra (a) and (c) correspond to the well-known silicate bands due, respectively, to the stretching and bending modes of the Si–O bonds. The broad and unstructured bands in Figs. 1a and 1c are characteristic of the amorphous state, whereas, the intermediate spectrum Fig. 1b, clearly shows that extensive crystallization has taken place due to the appearance of distinct peaks in the 15–40  $\mu\text{m}$  region and new structure in the  $\sim 10$   $\mu\text{m}$  band.

Difficulties in extracting the exact band positions longward of 35  $\mu\text{m}$  (due to the detection limits of our spectrometer) and in analysing the second broad band at  $\sim 20$   $\mu\text{m}$  in the amorphous samples, due to its very broad structure and uncertainties in the baseline, lead us to focus our study on the evolution of the 10  $\mu\text{m}$  Si–O stretching band for a quantitative analysis, as explained later.

The crystalline silicate bands obtained after thin film crystallization are compared to those of olivine grains embedded in CsI in Fig. 2. The pellet used has the same dimensions as our other samples (3 mm diameter and  $\sim 0.25$  mm thickness). In Fig. 2a, we show the raw spectrum for olivine grains embedded in CsI and in Fig. 2b we show the spectrum of the thin film. Qualitatively a good spectral agreement between the two samples is obtained. However, a small band shift (less than 1%) is observed and is attributed to grain size and matrix effects in the CsI embedded sample. We also note that the bands in the crystalline olivine thin film are somewhat narrower.

As mentioned above a re-amorphization of the thin film was achieved by  $\text{He}^{+}$  irradiation. As expected, and as shown by Demyk et al. (2001), low energy  $\text{He}^{+}$  ion irradiation is sufficient to induce structural changes in the crystallized silicate. In fact, the spectrum given in Fig. 1c obtained after the  $\text{He}^{+}$  irradiation (see Sect. 2) reveals a completely amorphous structure.

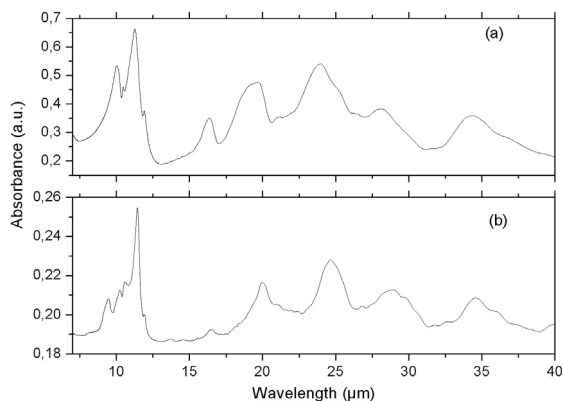


**Fig. 2.** IR spectra of: **a)** San Carlos olivine grains embedded in a CsI pellet, **b)** crystallized silicate thin film after annealing at 1050  $^{\circ}\text{C}$  for 30 min.

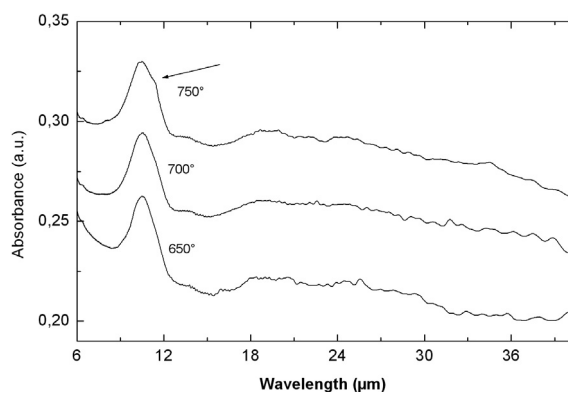


**Fig. 3.** The evolution of the silicate bands as a function of annealing time. The samples were annealed for 30 min at three different temperatures. The arrow indicates the position of the first crystalline silicate band to appear at  $\sim 11.4$   $\mu\text{m}$ .

### 3.1. Annealing results

Recrystallization of the thin film sample after  $\text{He}^{+}$  irradiation is performed by step-wise thermal annealing. We first annealed the sample for 30 min at a temperature of 650  $^{\circ}\text{C}$  and then for 30 min in 50  $^{\circ}\text{C}$  steps (650  $^{\circ}\text{C}$ , 700  $^{\circ}\text{C}$ , 750  $^{\circ}\text{C}$ ). The corresponding IR spectra are given in Fig. 3 where no significant evolution is seen from 650  $^{\circ}\text{C}$  to 700  $^{\circ}\text{C}$ . The growth of a band at  $\sim 11.4$   $\mu\text{m}$  ( $877$   $\text{cm}^{-1}$ ), that can be attributed to the onset of the formation of crystalline structure, is observed in the spectrum of the sample after annealing at 750  $^{\circ}\text{C}$  (1023 K). We then studied the evolution of the spectrum with annealing time at 750  $^{\circ}\text{C}$ . The spectra obtained for annealing times between 30 min and 20 h are shown in Fig. 4 where we observe the progressive growth of the crystalline bands. For each spectrum the corresponding annealing time is indicated in the figure.

### 3.2. Qualitative analysis

We now focus on the evolution of the silicate 10  $\mu\text{m}$  band. To a first approximation we can reasonably assume a linear baseline between 8.3 and 13.3  $\mu\text{m}$ . Figure 5 shows spectra after such a linear baseline subtraction, the corresponding annealing time for each spectrum is given in the legend.

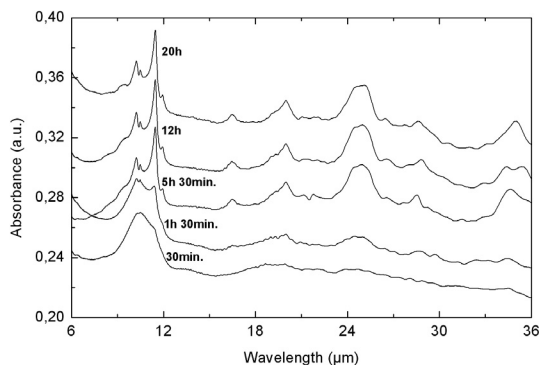


**Fig. 4.** The crystalline silicate band evolution as a function of annealing time (given for each spectrum) at 750 °C. For clarity we have shifted the 30 min, 5h30min and 12h spectra by  $-0.06$ ,  $-0.08$  and  $+0.02$ , respectively.

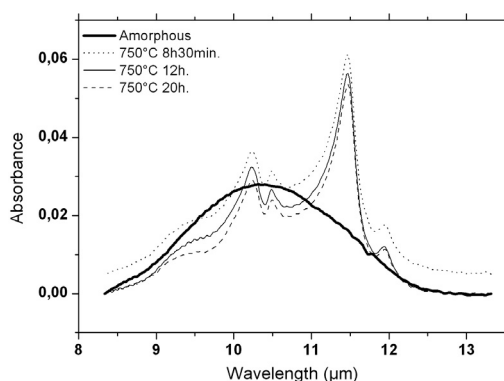


**Fig. 5.** The evolution of the 10  $\mu\text{m}$  silicate band in going from an initial amorphous state (thick solid line) to a final crystalline state: for 8h30min (dotted line), 12 h (thin solid line) and 20 h (dashed line) annealing times. The 8h30min spectrum has been shifted upward by 0.005 for clarity.

We now introduce the quantity  $t$  defined by the empirical relationship (Brucato et al. 1999; Fabian et al. 2000):

$$t = \nu^{-1} \exp\left(\frac{E_a}{kT}\right) \quad (1)$$

$t$  is a characteristic annealing time which is experimentally determined as the time after which no significant spectral changes are observed for a sample heated at a given temperature  $T$  (in Kelvin).  $E_a$  is the activation energy needed to reach the crystalline state from an amorphous one,  $k$  is the Boltzmann constant and  $\nu$  is a constant proportional to the mean vibrational frequency of the silicate lattice (Lenzuni et al. 1995). For magnesium silicates the mean value of  $\nu$  is  $2.0 \times 10^{13} \text{ s}^{-1}$  (Gail & Sedlmayr 1998), Brucato et al. (2002) used a value of  $2.5 \times 10^{13} \text{ s}^{-1}$ . In this work we use the intermediate value of  $(2.25 \pm 0.25) \times 10^{13} \text{ s}^{-1}$ .

Comparing the spectra obtained after the 8h30min, 12h and 20h annealing times (see Figs. 4 and 5) no further spectral evolution is observed. We can thus reasonably assume that the crystallization time  $t$  falls between 5h30min and 8h30min, we assume a value  $t = 7\text{h} \pm 1\text{h}30\text{min}$ .

Using Eq.(1) and taking into account the 5% and 11% uncertainties obtained for the temperature determination inside

the furnace and the  $\nu$  value, respectively, we deduce an activation energy value of  $E_a/k = 41\,700 \pm 2400 \text{ K}$ .

This value of the recrystallization activation energy after  $\text{He}^+$  irradiation falls between those determined elsewhere for  $\text{Mg}_2\text{SiO}_4$ . In fact, Hallenbeck et al. (1998) and Brucato et al. (2002) found 45 500 K and 40 400 K, respectively. However, our value is higher than 39 100 K, the value found by Fabian et al. (2000) for  $\text{Mg}_2\text{SiO}_4$  smoke-like nano-particles. The differences in these values may arise from the facts that, firstly, our sample preparation differs from those in the other cited works and, secondly, the presence of iron in the San Carlos olivine could modify the activation energy from that of a pure  $\text{Mg}_2\text{SiO}_4$  sample.

An examination of the spectra of the crystallized samples shown in Fig. 5 reveals a broad feature at  $\sim 9.2 \mu\text{m}$  ( $1087 \text{ cm}^{-1}$ ) that can be attributed to an amorphous  $\text{SiO}_2$  component (Nuth & Donn 1982). The presence of amorphous silica may be due to a selective evaporation of magnesium during the annealing in vacuum (Rietmeijer et al. 1986; Karner & Rietmeijer 1996 and Hallenbeck et al. 1998). The thin film studied here was also analyzed by transmission electron microscopy and the presence of an amorphous  $\text{SiO}_2$  phase was confirmed. We note that the crystallization temperature for fused silica ( $>1300 \text{ }^\circ\text{C}$ , Ainslie et al. 1962) is well above the maximum temperature used in our experiments. The results obtained in a follow-up study will be given in a forthcoming paper.

### 3.3. Quantitative analysis

In this section we investigate the mode of recrystallization in an irradiated sample by performing a systematic study of the crystalline silicate band evolution with the annealing time. We first synthesized a new sample using the same experimental protocol as described earlier. The IR spectrum shows that this sample was thicker than the first one by about 70%.

In order to completely amorphize this thicker sample we irradiated it with a higher energy (10 keV)  $\text{He}^+$  beam and a fluence of  $5 \times 10^{16} \text{ at/cm}^2$ . We used the TRIM implantation code (Ziegler et al. 1996) to verify that the entire bulk of the sample would be irradiated.

Our analytical procedure consists of the subtraction of a linear baseline between the adopted limits of the 10  $\mu\text{m}$  silicate band (taken to be 8.3 and 13.3  $\mu\text{m}$ ). We then normalize the spectra to the maximum absorbance in order to reduce errors and to avoid instrumental effects.

Firstly, we assume that the synthesized thin film sample obtained by evaporation is 100% amorphous and that a 100% crystalline silicate is obtained after annealing at 1050 °C for 30 min. A linear combination of these two spectra can then be used to model the band profile evolution as a function of the amorphous/crystalline ratio (see Fig. 6). From these profiles, we then determined the relationship between the band area and crystalline fraction in the sample.

Secondly, for each annealing step at 750 °C we determine the 10  $\mu\text{m}$  band area. Then from the derived relationship between band area and crystalline fraction, we estimated the crystalline fraction in the sample. This was done for annealing

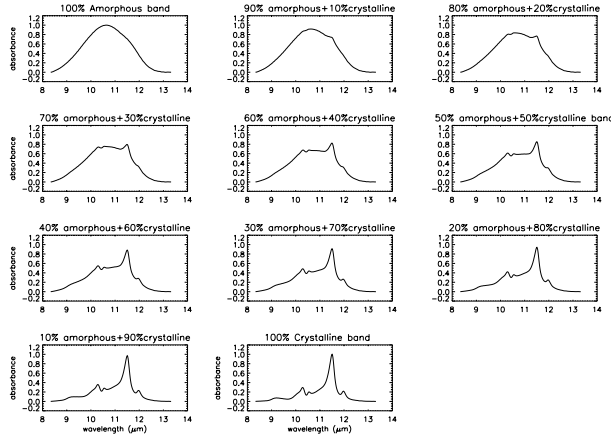


**Fig. 6.** The 10  $\mu\text{m}$  band evolution as a function of the amorphous/crystalline fraction. These profiles were obtained by using a linear combination of the amorphous and crystalline spectra. We assumed that the sample obtained by evaporation synthesis is 100% amorphous and that a 100% crystalline film is obtained after heating the sample at 1050  $^{\circ}\text{C}$  for 30 min.

**Table 1.** Crystalline fraction as a function of the annealing time at 750  $^{\circ}\text{C}$  (1023 K). For times longer than 14 000 s, a plateau is reached and the variation is due to the uncertainties in the method.

Time (s)	Crystalline fraction $x$
1800	33%
2700	40%
3600	50%
5400	68%
7200	75%
9000	77%
12 600	84%
14 400	91%
16 200	90%
18 000	89%

times between 30 min and 5 h, as shown in Table 1. Clearly the crystalline fraction varies between  $\sim 30\%$  and  $\sim 90\%$ .

A comparison of the 10  $\mu\text{m}$  band obtained after 20 h of annealing at 750  $^{\circ}\text{C}$  (Fig. 5) with the profiles given in Fig. 6 leads to an estimate of a mixture of 80% crystalline with 20% amorphous in the sample. This “less than 100% crystallinity” is correlated with the presence of the amorphous  $\text{SiO}_2$  band.

The relationship between the determined crystalline fraction  $x$  and the time  $t$  can be expressed by the isothermal Johnson-Mehl-Avrami kinetic equation (Avrami 1939, 1940, 1941)

$$x = 1 - \exp(-(Kt)^n) \quad (2)$$

where  $x$  is the fraction transformed at a given time  $t$  and at a particular temperature.  $n$  is the Avrami exponent, a number related to the geometric shape of the growing phase and the different crystallization mechanisms:  $n = 4$  corresponds to a volume nucleation with three dimensional growth;  $n = 3$  to a volume nucleation with two dimensional growth;  $n = 2$  to a volume nucleation with one dimensional growth;  $n = 1$  to a surface nucleation with one dimensional growth from the surface to the interior.  $K$  is a temperature-dependent rate constant

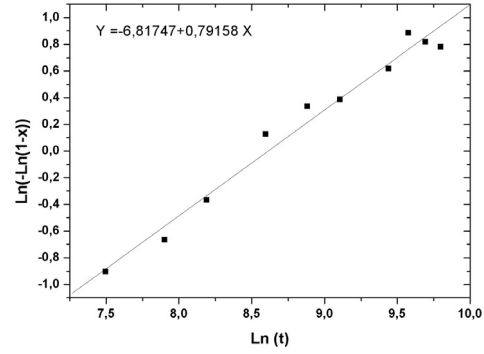


**Fig. 7.** The Avrami curve for the sample recrystallized at 1023 K. The symbols represent the data given in Table 1 and the line is a linear fit to the data. The equation of the line is also given.

(Arrhenius dependence) which includes the nucleation rate and the rate constant for crystal growth.

$$K = K_0 \exp\left(-\frac{Q}{RT}\right) \quad (3)$$

where  $Q$  is the activation energy for recrystallization,  $K_0$  is the pre-exponential constant (related to the Debye frequency) and  $R$  is the gas constant.

The Avrami equation can also be plotted in its logarithm form, i.e.,

$$\text{Ln}(-\text{Ln}(1-x)) = n\text{Ln}(K) + n\text{Ln}(t). \quad (4)$$

The Avrami exponent  $n$  can be calculated from the slopes of the curve  $\text{Ln}(-\text{Ln}(1-x))$  versus  $\text{Ln}(t)$ , where  $x$ , the crystalline fraction, is determined experimentally.

In Fig. 7 we report the data given in Table 1 and a linear fit to these data (solid line). According to Eq. (4) we can see that the Avrami exponent (corresponding to 0.79, the slope of the line) in our experiments is close to 1, suggesting that the nucleation of the crystalline material began at the surface and that the growth was unidirectional. This nucleation and crystal growth mechanism is not surprising since the geometry of the starting sample, a thin film, strongly favors the role of the surface.

The fit to the data also leads to a determination of the activation energy, here denoted as  $Q$ . The data given in Fig. 7 yield a value of 40 142 K for the ratio  $Q/R$  which is close to the value determined from our qualitative analysis of the spectra and well within the error bars given above.

#### 4. Discussion and conclusions

We have simulated in the laboratory processes in the life-cycle of silicate grains in interstellar and circumstellar media when they are exposed to ion irradiation and thermal annealing. As is well-known, the heating of an amorphous Mg-rich olivine-type silicate to temperatures exceeding 1000 K is sufficient to crystallize the sample in a few minutes. In fact, thermal diffusion is the principal process which leads to a re-arrangement of the structural units resulting in the formation of a long range order characterized by narrow IR bands, in contrast to the broad bands characteristic of an amorphous sample. As shown by

Demyk et al. (2001) and Carrez et al. (2002), He<sup>+</sup> irradiation results in an amorphization of the material and to He implantation which results in a large defect concentration in the sample. The formation of defects could, in theory, facilitate recrystallization in cold environments, as suggested by Fabian et al. (2000). However, our results show that there is no direct correlation between prior ion irradiation and a “fast” recrystallization of amorphous olivine-type silicates. Such a “low temperature” crystallization mechanism was proposed by Molster et al. (1999).

From a qualitative analysis of our IR spectra we have determined a value for the activation energy of re-crystallization for an He<sup>+</sup>-irradiated olivine-type silicate. The good agreement between our result and those published elsewhere for the activation energy of crystallization for non-irradiated amorphous silicates suggests that He<sup>+</sup> irradiation does not modify the silicate crystallization process. A more quantitative analysis of the 10 μm silicate band suggests, firstly, that the nucleation of the crystalline domains in silicates occurs from the surface of the amorphous silicate. Secondly, the use of the Avrami relationship leads to an estimate of the activation energy which is also close to previously-determined values of the activation energy for crystallization. This second determination of the activation energy of crystallisation (sample irradiated at 10 keV versus 5 keV for the first sample analysed qualitatively) corroborates the fact that pre-irradiation can not be responsible for stimulating the recrystallization of amorphous silicates.

For the crystalline dust observed in astrophysical environments such as around young stars, and in some comets, where the crystalline silicates are seen mixed with low temperature interstellar ices, pre-irradiation in the ISM can not explain the preferential recrystallization. It is thus necessary to invoke a recycling of the material between the hot inner parts and the cold outer parts of the nebula, followed by a subsequent condensation of the ices in the cold outer regions.

Our results concern only olivine-type silicates irradiated with He<sup>+</sup> ions at two energies and annealed at 750 °C. It is necessary to investigate other silicate-type minerals subjected to irradiation by other ions and annealing in order to definitively conclude that ion-irradiated silicates do not show modified thermodynamical properties. In the ISM, including molecular clouds, the silicates are amorphous before their incorporation into young stellar environments where they can be partially in crystalline form. Thus, the crystallisation must have occurred in-situ close to young stars where some fraction of the dust must have been heated to temperatures of at least 1030 K. Malfait et al. (1999) reported the existence of two different dust populations in the circumstellar dust disk of the young star HD 142527. These populations consist of a warm component, mainly composed of crystalline silicate with a temperature ranging from 500 to 1500 K, and a cold crystalline silicate component (30–60 K) associated with the hydrated silicates that are incorporated into their model. This seems to be consistent with the idea of cycling and mixing in circumstellar disks.

*Acknowledgements.* The authors would like to thank D. Le Du for having performed the irradiation experiments at the CSNSM Orsay.

Z. Djouadi is grateful to the PNP-CNRS program for funding this experimental work.

## References

- Ainslie, N. G., Morelock, C. R., & Turnbull, D. 1962, in Symposium on Nucleation and Crystallization in Glasses and Melts, ed. M. K. Reser, G. Smith, & H. Insky, 97, American Ceramic Society, Columbus
- Avrami, M. 1939, *J. Chem. Phys.*, 7, 1103
- Avrami, M. 1940, *J. Chem. Phys.*, 8, 212
- Avrami, M. 1941, *J. Chem. Phys.*, 9, 177
- Brucato, J. R., Colangeli, L., Mennella, V., et al. 1999, *A&A*, 348, 1012
- Brucato, J. R., Mennella, V., Colangeli, L., et al. 2002, *PSS*, 50, 829
- Brucato, J. R., Strazzulla, G., Baratta, G., et al. 2004, *A&A*, 413, 395
- Carrez, P., Demyk, K., Cordier, P., et al. 2002, *Meteor. Planet. Sci.*, 37, 1599
- Chauvin, N., Chauvin, N., Dayras, F., Le Du, D., & Meunier, R. 2004, *Nucl. Inst. Meth. A*, 521, 149
- Colangeli, L., Henning, Th., Brucato, J. R., et al. 2003, *A&AR*, 11, 97
- Crovisier, J., Leech, K., Bockelee-Morvan, D., et al. 1997, *Science*, 275, 1904
- Demyk, K., Jones, A. P., Dartois, E., et al. 1999, *A&A*, 349, 267
- Demyk, K., Carrez, P., Leroux, H., et al. 2001, *A&A*, 368, L38
- Demyk, K., d’Hendecourt, L., Leroux, H., et al. 2004, *A&A*, 420, 233
- Fabian, D., Jaeger, C., Henning, Th., et al. 2000, *A&A*, 364, 282
- Gail, H. P., & Seldmeyer, E. 1998, in *The Molecular Astrophysics of Stars and Galaxies*, ed. T. W. Hartquist & D. A. Williams (Oxford: Clarendon Press), 285
- Hallenbeck, S. L., Nuth, J. A., & Daukantas, P. L. 1998, *Icarus*, 131, 198
- Hanley, L., & Sinnott, S. B. 2002, *Surf. Sci.*, 500, 500
- Herlin, N., Bohn, I., Reynaud C., et al. 1998, *A&A*, 330, 1127
- Jaeger, C., Molster, F. J., Dorschner, J., et al. 1998, *A&A*, 339, 904
- Jaeger, C., Fabian, D., Schrempel, F., et al. 2003, *A&A*, 401, 57
- Jaeger, C., Dorschner, J., Mutschke, H., et al. 2003, *A&A*, 408, 193
- Jones, A. P. 2000, *JGR-Space Phys.*, 105, 10257
- Karner, J. M., & Rietmeijer, F. J. M. 1996, *LPS*, 27, 647
- Kemper, F., Waters, L. B. F. M., de Koter, A., et al. 2001, *A&A*, 369, 132
- Kemper, F., Vriend, W. J., & Tielens, A. G. G. M. 2004, *ApJ*, 609, 826
- Lenzuni, P., Gail, H., & Henning, T. 1995, *ApJ*, 447, 848
- Malfait, K., Waelkens, C., Waters, L. B. F. M., et al. 1998, *A&A*, 332, L25
- Malfait, K., Waelkens, C., Bouwman, J., et al. 1999, *A&A*, 345, 181
- Molster, F. J., Yamamura, I., Waters, L. B. F. M., et al. 1999, *Nature*, 401, 563
- Molster, F. J., Waters, L. B. F. M., & Tielens, A. G. G. M. 2002, *A&A*, 382, 222
- Nuth, J. A., & Donn, B. 1982, *ApJ*, 257, L103
- Rietmeijer, F. J. M., Nuth, J. A., & Mackinnon, I. D. R. 1986, *Icarus*, 66, 211
- Rietmeijer, F. J. M., Nuth, J. A., & Karner, J. M., 1999, *ApJ*, 527, 395
- Vogelgesang, R., Alvarenga, A. D., Hyunjung Kim, et al. 1998, *Phys. Rev. B*, 58, 5408
- Waters, L. B. F. M., Molster, F. J., de Jong, T., et al. 1996, *A&A*, 315, L361
- Wooden, D. H., Harker, D. E., Woodward, C. E., et al. 1999, *ApJ*, 517, 1034
- Wooden, D. H., Woodward, C. E., & Harker, D. E. 2004, *ApJ*, 612, L77
- Ziegler, J. F., Biersack, J. P., & Littmark, U. 1996, *The Stopping and Range of Ions in Solids (USA)*, New York: Pergamon Press)